Rapidity of the Change of the Kohlrausch Exponent of the α-Relaxation of Glass-Forming Liquids at T_B or T_β and Consequences

C. León and K. L. Ngai*

Naval Research Laboratory, Washington, D.C. 20375-5320

Received: September 17, 1998; In Final Form: December 2, 1998

Stickel, Fischer, and Richert [*J. Chem. Phys.* **1996**, *104*, 2043] found the temperature dependence of the α-relaxation time, $\tau_\alpha(T)$, of many small-molecule glass-forming liquids undergoes a change at a characteristic temperature, T_B. On the lowering of temperature, $\tau_\alpha(T)$ changes from one Vogel−Fulcher−Tammann (VFT) dependence, VFT_h, that holds for $T > T_B$ to another VFT dependence, VFT_l, or a non-VFT dependence, $nVFT_l$, for $T < T_B$. In glass-formers, which exhibit a β-relaxation of the Johari−Goldstein type, extrapolation of the Arrhenius temperature dependence of its relaxation time, $\tau_\beta(T)$, indicates that it tends to merge into the α-relaxation at a temperature, T_β. Stickel et al. found also that T_B coincides with T_β. This work augments these important findings by showing that, for fragile glass-formers, on decreasing temperature there is at $T_B \approx T_\beta$ a rapid steplike change of the Kohlrausch−Williams−Watts exponent, $(1 - n)$, of the primary α-relaxation correlation function, $\exp[-(t/\tau_\alpha)^{1-n}]$. The size of the steplike change of different glass-formers decreases proportionately with decreases in the value of $n(T_g)$ at the glass transition temperature T_g and in the difference between VFT_h and VFT_l or $nVFT_l$, after these functions are extended to a common temperature range above and below T_B. These correlations are interpreted as due to the onset of significant increase of cooperativity at and below $T_B \approx T_\beta$ as indicated by the rapidity of the increase of $n(T)$ in the framework of the coupling model. If one compares different glass-formers at the same value of the ratio, T_B/T, the interpretation corroborates the experimental fact that a larger steplike increase of $(1 - n)$ across T_B gives rise to larger separation between the logarithm of the α and β relaxation times. The fact that T_β nearly coincides with T_B is also explained. For $(T_B/T) > 1$, the difference, $\log[\tau_\alpha(T_B/T)] - \log[\tau_\beta(T_B/T)]$, remains small for strong glass-formers with small $n(T_g)$ and small step increase of $(1 - n)$ across T_B. As a result, a β-relaxation peak or shoulder cannot be resolved from the α-relaxation peak and observed as a wing on the high-frequency side of the α-relaxation peak. This interpretation can further explain the origin of the success of the Dixon−Nagel scaling of the dielectric loss data of glass-formers.

1. Introduction

The glass transition phenomenon is widespread in materials of diverse chemical compositions and physical structures and has been a subject of research for many years.[1,2] The ultimate goal of most researchers is to understand the molecular dynamics and their changes over a broad temperature range in which the structural relaxation time changes from the microscopic regime of the order of picoseconds to macroscopic times of the order of days. This lofty goal is hard to achieve because several factors have a bearing on the glass transition phenomenon. Possible factors include the specific volume, configuration entropy, intermolecular constraints, and many-body interactions (cooperativity). Moreover, these factors change with temperature and make the treatment of the problem even more difficult. Most treatments cannot consider all the factors all at one time, and it is not difficult to understand that none of them can capture all the features of the glass transition phenomenon. While a complete theory of glass transition will not be available for some time, a modest but worthwhile undertaking is to isolate one factor such as cooperativity and use a viable theoretical approach that can account for its effect to bring some predictions to compare with experimental data. This approach cannot be a complete theory of glass transition but, if successful, is the basis on which to build one by incorporating other factors. The coupling model[3,4] when applied to the molecular dynamics of glass-forming materials is an example of such an approach that tries to account for the effects coming only from the many-body cooperative dynamics.

In this work the coupling model is brought to address the interesting findings in a series of papers by Stickel et al.,[5,6] Hansen et al.,[7,8] and Richert and Angell[9] that the temperature dependence of the α-relaxation time, $\tau_\alpha(T)$, of many small molecule glass-forming liquids undergoes a change at a characteristic temperature, T_B. On the lowering of temperature, $\tau_\alpha(T)$ changes from one Vogel−Fulcher−Tammann (VFT) dependence, VFT_h,

$$\log \tau_\alpha(T) \equiv VFT_h(T) = A_h + B_h/(T - T_{0h}) \qquad (1)$$

for $T > T_B$ to another VFT dependence, VFT_l,

$$\log \tau_\alpha(T) \equiv VFT_l(T) = A_l + B_l/(T - T_{0l}) \qquad (2)$$

or a non-VFT dependence, $nVFT_l$, that holds for $T < T_B$. In glass-formers, which exhibit a β-relaxation of the Johari−Goldstein kind, extrapolation of the Arrhenius temperature dependence of its relaxation time, $\tau_\beta(T)$, indicates that it tends to merge into the α-relaxation at a temperature, T_β. Stickel et al. found also that T_B is nearly the same as T_β.[5−9] In our present work we point out from dielectric data of fragile glass-formers that on decreasing temperature at $T_B \approx T_\beta$ there is a rapid

10.1021/jp983756h CCC: $18.00
Published on Web 01/22/1999

steplike change of the stretch exponent, $(1 - n)$, of the primary α-relaxation Kohlrausch−Williams−Watts (KWW)[10,11] correlation function, $\exp[-(t/\tau_\alpha)^{1-n}]$. The size of the steplike increase of n, proportional to the value of $n(T_g)$ at the glass transition temperature T_g, turns out to correlate with the difference between VFT_h and VFT_l or $nVFT_l$, after these functions are extended to a common temperature range above and below T_B. Strong glass-formers with small $n(T_g)$ show weak increase of n across T_B and minor difference between VFT_h and VFT_l. These experimental facts and the correlations between them are interpreted to originate from onset of significant increase of cooperativity at T_B in the framework of the coupling model,[3,4] where it is measured by the rapidity of the increase of the coupling parameter n.

Furthermore, on comparison of different glass-formers at the same value of the ratio, T_B/T, the interpretation corroborates the experimental fact that a larger steplike increase of $(1 - n)$ across T_B gives rise to larger separation between the logarithm of the α and β relaxation times. The difference, $\log[\tau_\alpha(T_B/T)] - \log[\tau_\beta(T_B/T)]$, is small for strong glass-formers with small $n(T_g)$ and small step increase in $(1 - n)$ across T_B. As a result, neither a β-relaxation peak nor a shoulder can be resolved from the α-relaxation peak, and the β-relaxation can at best be observed as a wing on the high-frequency side of the α-relaxation peak. This interpretation of the dielectric spectra is reinforced by a comparison with that of cyclooctanol. The dielectric spectrum of cyclooctanol has a similar shape, but special circumstance enabled the β-relaxation peak to be resolved and support our interpretation.

Finally, this interpretation of the dielectric relaxation spectra of glass-forming liquids which do not clearly exhibit a β relaxation peak or shoulder is further used to explain the origin of the success of the Dixon−Nagel scaling[12,13] of the dielectric loss data of small molecules glass-formers, particularly those having smaller $n(T_g)$ such as glycerol, propylene glycol, and cyclooctanol.

2. Rapidity of the Increase of n across T_B

Experimental data on the dielectric dispersion of the primary α-relaxation are available and were presented in refs 5 and 6. There, w, the full widths at half-maximum of the dielectric loss peak normalized to that of an ideal Debye loss peak, were given as a function of temperature for many glass-formers. The dielectric dispersion of the α-relaxation of most glass formers are adequately fitted by the Fourier transform of the time derivative of the KWW correlation functions, $\exp[-(t/\tau_\alpha)^{1-n}]$. An approximate relation between w and n in the KWW exponent given by Dixon[13] has the form

$$n \equiv 1 - \beta_{KWW} = 1.047(1 - w^{-1}) \qquad (3)$$

In previous works, the temperature variation of $(1 - n)$ or w in relation to T_B and its significance has not been emphasized. In the coupling model n, the coupling parameter, is a measure of the degree of intermolecular cooperativity and is one of the factors that determine the temperature dependence of τ_α (see section 3). Therefore a crossover of temperature dependence of τ_α at T_B suggests there could be a concomitant change in the temperature dependence of $(1 - n)$. For this reason we convert the dielectric data of $w(T)$ to $n(T)$ according to eq 3 and plot $n(T)$ against the scaled reciprocal temperature, T_B/T. In this plot (Figure 1a) we can compare the data of four different glass-formers, *o*-terphenyl (OTP), salol, glycerol, and propylene glycol (PG). OTP and salol are fragile glass-formers with larger values of $n(T_g)$ and fragility index, m.[14] Glycerol and PG on the other hand are intermediate liquids with smaller values of $n(T_g)$ and m. These parameters together with T_B for these four glass-

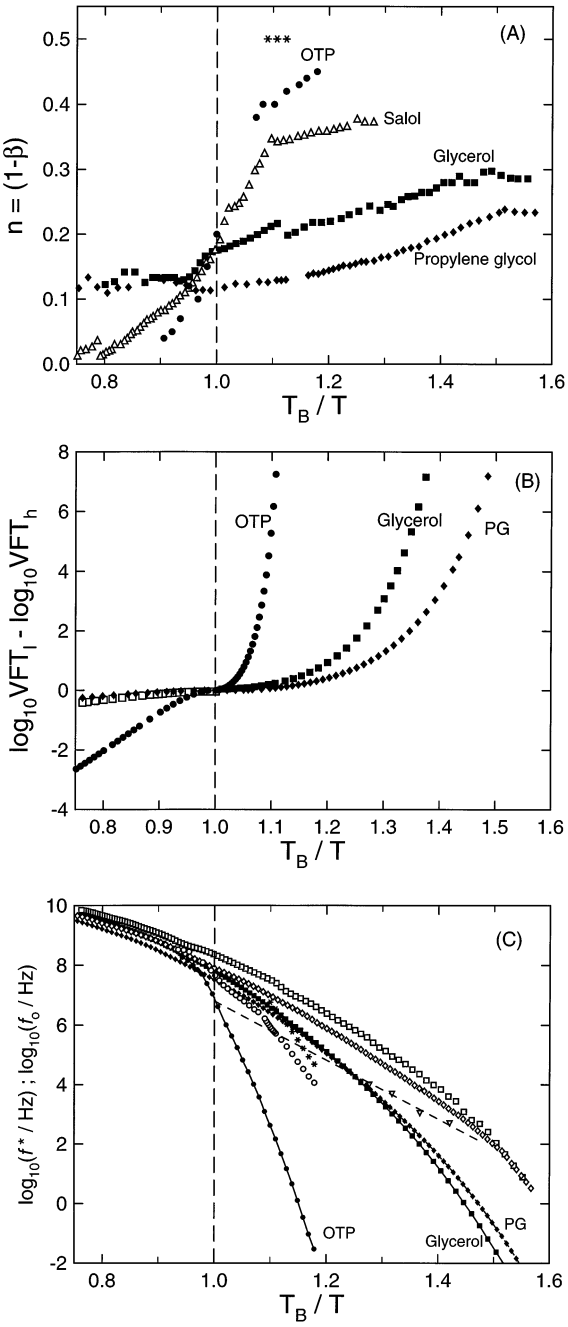

Figure 1. (a) Normalized reciprocal temperature, T_B/T, dependence of n in the exponent, $(1 - n)$, of Kohlrausch relaxation function of four glass-forming liquids, OTP (●, from dynamic light scattering; ∗, from dielectric relaxation), salol (△ from dielectric), glycerol (■), and propylene glycol (♦), plotted as a function of the scaled reciprocal temperature, T_B/T. (b) Normalized reciprocal temperature, T_B/T, dependence of the difference $\Delta(T)$ between the two Vogel−Fulcher−Tammann expressions (eqs 1 and 2) of the α-relaxation time defined by eq 4 on the scaled reciprocal temperature, T_B/T, for OTP (●), propylene glycol (◆), and glycerol (■). (c) Dielectric α-relaxation times of OTP (●), glycerol (■) and propylene glycol (◆), and the corresponding primitive α-relaxation times of OTP (○, calculated by using $(1 - n)$ from light scattering; ∗, by using $(1 - n)$ from dielectric relaxation), glycerol (□) and propylene glycol (◇). All quantities are plotted as a function of T_B/T. The dielectric β-relaxation times of OTP (▽) measured below T_g are extrapolated to higher temperatures by assuming that throughout it has an Arrhenius temperature dependence (dashed straight line). The extrapolation indicates that $T_B \approx T_\beta$.

TABLE 1: Characteristic Parameters of the Four Glass-Forming Liquids in Decreasing Order of Fragility, *m*, with All Temperatures in Units of K

glass-former	T_g	T_B	T_β	$n(T_g)$	m
OTP	246	290[a]	290	0.45[b]	81[e]
				0.50[c]	
salol	220	265[a]	na	0.38[d]	63[e]
glycerol	190	285[a]	na	0.3[d]	53[e]
propylene glycol	167	280[a]	na	0.23[d]	52[e]

[a] Stickel, F. Ph.D. Thesis, Mainz University, Shaker, Aachen, Germany, 1995. [b] From photon correlation spectroscopic data of: Steffen, W.; Patkowski, A.; Glaesser, H.; Meier, G.; Fischer, E. W. *Phys. Rev. E* **1994**, *49*, 2992. Steffen, W. Ph.D. Thesis, Mainz University, Shaker, Aachen, Germany, 1993. [c] From dielectric relaxation data of H. Wagner and R. Richert (unpublished). [d] Converted from the data of the width, *w*, of dielectric loss peak given by Stickel in his thesis by using eq 3. [e] Böhmer, R.; Ngai, K. L.; Angell, C. A.; Plazek, D. J. *J. Chem. Phys.* **1993**, *99*, 4201.

formers are shown in Table 1. OTP has low dielectric relaxation strength, and its dispersion is more difficult to obtain. The widths *w* of OTP obtained from some very recent dielectric relaxation data[15a] at temperatures of 266, 262, and 258 K give $n \approx 0.5$. Higher temperature dielectric data of OTP are not available, and we use photon correlation spectroscopy and depolarized light scattering data[15b] to obtain $n(T)$ of OTP. There are slight differences between $n(T)$ from dielectric relaxation and light scattering data. However, this difference does not alter the trend, which will be discussed next.

It can be seen by inspection of Figure 1a that, among the four glass-formers, the most fragile OTP having the largest $n(T_g)$ exhibits the most rapid rise of $n(T)$ across $T_B/T = 1$. A less steep rise of $n(T)$ across $T_B/T = 1$ is still visible in salol, which ranks second according to $n(T_g)$ and m. The rise of $n(T)$ across $T_B/T = 1$ is weak for glycerol, and the rise disappears for PG. This systematic dependence of the variation of $n(T)$ across $T_B/T = 1$ on $n(T_g)$, on first sight, may not be too much a surprise because $n(T)$ has to rise from nearly zero value at high temperatures to $n(T_g)$ in crossing T_B. However this may not be so trivial because when plotting $n(T)$ against T_B/T there is no guarantee that the rapidity of the rise of $n(T)$ across $T_B/T = 1$ is still proportional to $n(T_g)$. Next we show that the variation of $n(T)$ across $T_B/T = 1$ is correlated with the difference $\Delta(T)$ between the two Vogel−Fulcher−Tammann expressions (eqs 1 and 2) defined by

$$\Delta(T) \equiv VFT_h(T) - VFT_l(T) \tag{4}$$

after the two functions are extended to a common temperature range above and below T_B. $\Delta(T)$ quantifies the change from $VFT_h(T)$ to $VFT_l(T)$ of the temperature dependence of $\tau_\alpha(T)$ across T_B. Earlier Richert and Angell[9] considered instead the scalar quantity $\kappa = B_l/B_h$. In Figure 1b $\Delta(T)$ is plotted against T_B/T for OTP, glycerol, and PG. Salol is not included because below T_B the temperature dependence of its $\tau_\alpha(T)$ does not obey the VFT form. The scaled reciprocal temperature plot shows that the variation of $\Delta(T)$ is most rapid for OTP and decreases when going to glycerol and PG. In a comparison of Figure 1a with Figure 1b, the variation of $\Delta(T)$ with T_B/T is clearly correlated with the variation of $n(T)$ with T_B/T. The glass-former having a larger $n(T_g)$ has a more rapid variation of both quantities with T_B/T. This correlation suggests that the change in slope of $\tau_\alpha(T)$ at T_B may originate from the onset of a rapid change in $n(T)$. If $n(T)$ is a measure of cooperativity, then the rapidity of its change across T_B is an indication of how significant is the increase of cooperativity at temperatures below T_B. Glass-formers such as OTP in which a β-relaxation peak has been resolved, T_B is nearly the same as the $\alpha-\beta$ bifurcation temperature, T_β. Naturally, this coincidence of T_B with T_β raises the possibility that the location as well as the dynamics of the β-relaxation is controlled also by the variations of $n(T)$ or $\tau_\alpha(T)$ across T_B. It was recently pointed out[16] on both empirical and theoretical grounds that strong glass-formers with small values of $n(T_g)$ do not show a β-relaxation peak or shoulder in the dielectric relaxation spectrum.[16] A specific question on β-relaxation dynamics is whether the fact that a β-relaxation peak or shoulder has not been resolved in glycerol, PG, and other strong liquids[16] has anything to do with the slow variations of $n(T)$ or $\tau_\alpha(T)$ across T_B and the small values of $n(T_g)$ found in these nonfragile glass-formers? To meaningfully discuss these issues and answer the questions, a theoretical framework is needed. In the sections to follow the coupling model is employed for this purpose.

3. Location of the Johari−Goldstein β-Relaxation

Before proceeding to give a theoretical interpretation of the experimental facts summarized in Figures 1a−c and to answer the questions they raise, it is necessary to give a brief summary of the coupling model. In the coupling model (CM),[3,4,16] there exists a temperature-insensitive crossover time t_c with a magnitude determined by the strength of the intermolecular interaction. At times shorter than t_c, the basic molecular units relax independently of each other and exponentially (i.e., via the primitive α-relaxation mode) according to the normalized correlation function

$$\phi(t) = \exp[-(t/\tau_0)] \quad t < t_c \tag{5}$$

where τ_0 is the primitive α-relaxation time. At times longer than t_c, the intermolecular interactions (i.e. cooperativity) slow the relaxation and the averaged correlation function assumes the Kohlrausch stretched exponential form

$$\phi(t) = \exp[-(t/\tau_\alpha)^{1-n}] \qquad t > t_c \tag{6}$$

Continuity of $\phi(t)$ at t_c leads to the relation

$$\tau_\alpha = [t_c^{-n}\tau_0]^{1/(1-n)} \tag{7}$$

that relates the two times. Existence of a rather sharp crossover time has been shown by simple Hamiltonian models that exhibit chaos.[3,4] Experimental evidences for the existence of such a crossover at a time $t_c \approx 2$ ps come from quasi-elastic neutron scattering measurements in poly(vinyl chloride) (PVC),[18] poly(isoprene) (PI), and polybutadiene (PB)[19] performed at temperatures high above T_g where τ_α becomes short and of the order of 10 ps or less. Under this condition, the primitive α-relaxation decaying linear exponentially dominates the time dependence of $\phi(t)$ and is clearly evident from the relaxational part of the experimental data. There are also evidences for the crossover at $t_c \approx 2$ ps from analysis of molecular dynamics data of OTP,[20] polyethylene,[21,22] and polystyrene[23] and high-frequency dielectric measurement of a molten salt, CKN.[24] When applied to the glass transition problem, the dependence of the primitive α-relaxation time on temperature $\tau_0(T)$ is relegated to the other factors mentioned in the Introduction and not given. Although eq 7 takes us from $\tau_0(T)$ to $\tau_\alpha(T)$, taking care of the effect of slowing down by cooperative many-body dynamics, yet the coupling model at this stage is not a complete theory of glass transition because the temperature dependence of $\tau_0(T)$ is not obtained in the model.

The β-relaxation having characteristics such as Arrhenius temperature dependence of its relaxation time has been considered to be simple molecular motions that is not cooperative in nature.[17,25−28] Thus, in this respect the β-relaxation bears some resemblance to the primitive α-relaxation. However, they cannot be exactly the same otherwise the former like the latter will be slowed by intermolecular interactions to become the cooperative α-relaxation observed at longer times. From this similarity it is expected that $\tau_\beta(T)$ and $\tau_0(T)$ may be comparable in order of magnitude. This expectation was also made by Angell in one of his recent review of the dynamics of glass transition[29] and has recently been shown to be true for many glass-formers.[16] To compare the experimental values of $\tau_\beta(T)$ in materials where the β-relaxation is found with $\tau_0(T)$, the latter is calculated as a function of temperature from the experimental values of $\tau_\alpha(T)$ and $(1 - n(T))$ by solving the equation

$$\tau_0(T) = t_c^{\,n}[\tau_\alpha(T)]^{1-n} \tag{8}$$

with $t_c = 2$ ps. The result of $\tau_0(T)$ for OTP together with the experimental data of $\tau_\alpha(T)$ are shown as the open and solid circles in Figure 1c. The figure shows the extrapolated values of $\tau_\beta(T)$ (dashed straight line) from experimental data at lower temperatures (open triangles) are remarkably close (within approximately 1 order of magnitude) to $\tau_0(T)$ as anticipated by the resemblance between the two processes. It is worth to emphasize once more that the value of $t_c = 2$ ps used to calculate the solid line is not arbitrary and had been predetermined by experiment.[18−24] Similarly, $\tau_0(T)$ for glycerol and PG are calculated from their respective experimental values of $\tau_\alpha(T)$ and $(1 - n(T))$. The $\tau_\alpha(T)$ of glycerol and PG are shown in Figure 1c as solid squares and diamonds, respectively. The calculated values of $\tau_0(T)$ for glycerol and PG are shown as open squares and diamonds, respectively. One can see that the separation between $\tau_0(T)$ and $\tau_\alpha(T)$ in glycerol and PG is significantly smaller than in OTP. Within the temperature range of the experimental data in Figure 1c, the maximum separation between them near T_g is less than 3 decades for PG, compare with about 6 decades for OTP. At higher temperatures and the same value of T_B/T, the separation in PG is drastically smaller than in OTP. Assuming that $\tau_\beta(T)$ is comparable in order of magnitude to $\tau_0(T)$ in glycerol and PG as suggested by the example of OTP here[16] and other glass-formers including cyclooctanol[30,31] to be discussed next, we come to the conclusion that $\tau_\beta(T)$ is located close to $\tau_\alpha(T)$ in glycerol and PG. The dielectric strength of the α-relaxation is stronger than that of the β-relaxation. This together with the proximity of the most probable relaxation times of these two relaxation processes in glycerol and PG cause the β-relaxation peak in these glass-formers to be unresolved from the dominant α-peak and contributing only a high-frequency wing to the dielectric α-loss peak.[32−34] Even at temperatures below T_g, $\tau_\beta(T)$ becomes quite long and the dispersion so broad to make resolution of its peak difficult if not impossible.

This interpretation has support from the plastic crystal cyclooctanol.[30,31] The dielectric relaxation data of cyclooctanol resemble strongly that of glycerol and PG, and all of them can be scaled in the manner proposed by Dixon−Nagel to the same master curve.[30,31] The significance of the Dixon−Nagel scaling will be discussed further in the next section. The $\epsilon''(f)$ data show only the high-frequency wing, $C_1 f^{-\sigma}$, over and above the KWW fit, but no peak to indicate the presence of a β-relaxation. By studying dielectric relaxation of cyclooctanol in both the disordered and ordered states, Brand et al.[31] were able to resolve the β-relaxation peak. The existence of the β-relaxation peak is confidently established because in the ordered state the α-relaxation process is suppressed and the β-relaxation peak shows up clearly, shifting to higher frequencies with increasing temperature. The β-relaxation peak has approximately the Cole−Cole functional form,[35] and Brand et al. demonstrated that the high-frequency wing in the $\epsilon''(f)$ data of the supercooled, orientationally disordered phase arises from the superposition of the α-relaxation peak and the β-relaxation peak. Although Brand et al. fitted the α-relaxation peak to a Cole−Davidson form,[36] the results are not changed had they fitted the same to the KWW form. The temperature dependences of $\tau_\alpha(T)$ and $\tau_\beta(T)$ are depicted in Figure 2. The KWW exponent, β_{KWW}, of cyclooctanol was determined by Brand et al. as a function of temperature and its values are used via eqs 3 and 8 with $t_c = 2$ ps to calculate $\tau_0(T)$. The results compare well with $\tau_\beta(T)$ (see Figure 2) and support the thesis that $\tau_0(T)$ is a good approximant to $\tau_\beta(T)$ for temperatures above T_g as suggested for glycerol and PG. The strong resemblance of the $\epsilon''(f)$ data of cyclooctanol to other strong liquids suggests that the latter can also be explained by the presence of a β-relaxation that bears similar relation to the α-relaxation peak as in the former. In fact Lunkenheimer[37] was successful in fitting the $\epsilon''(f)$ data of glycerol in the manner as done for cyclooctanol by taking into account of a β-relaxation peak that has the Cole−Cole form. Therefore these cyclooctanol results strengthen the proposal that the β-relaxation peak or shoulder in nonfragile glass-formers in Figure 1 not being observed at all temperatures is due to their $\log[\tau_\beta(T)]$ being too close to $\log[\tau_\alpha(T)]$ as suggested by the locations of the calculated $\tau_0(T)$ for glycerol and PG in Figure 1c.

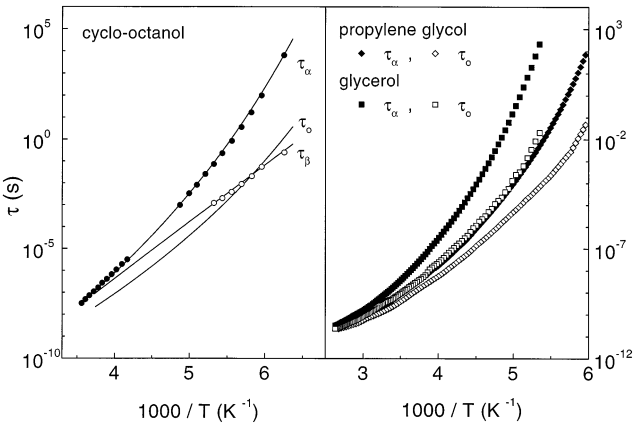

Figure 2. Left panel of the figure shows the temperature dependences of the relaxation times, τ_α and τ_β, of the α- and the β-relaxations, respectively, of cyclooctanol. Data are taken from Brand et al. The primitive relaxation time τ_0 of the α-relaxation, obtained by calculation from eq 8, is also shown in the same plot. The right panel of the figure shows the measured α-relaxation time, τ_α, and the corresponding calculated primitive α-relaxation times, τ_0, of glycerol and propylene glycol. Note the similarity of the relation between τ_α and τ_0 in these nonfragile liquids and in cyclooctanol. This similarity suggests that the β-relaxation times of glycerol and propylene glycol are positioned near τ_0, as in cyclooctanol.

We conclude this section by the remark that, empirically as well as can be considered as consequences of the coupling model, the rapidity of the variation of $n(T)$ across T_B in concert with the size of $n(T_g)$ determine several other features of the α and β relaxations of glass-formers. These features include the magnitudes of (1) the difference $\Delta(T)$ defined by eq 4 as a function of the scale reciprocal temperature T/T_B (see Figure 1b) and (2) the separation between the α and β relaxation times defined by $[\log(\tau_\alpha) - \log(\tau_\beta)]$ also as a function of T/T_B. In the coupling model the quantity $n(T)$ is the coupling parameter

which is a measure of the effects of intermolecular constraints or the degree of cooperativity. Therefore in the framework of the coupling model the observed changes of properties of relaxation across T_B are interpreted to be consequences of the onset of any significant increase of cooperativity at T_B.

For all the glass-formers discussed in this work, there is insignificant cooperativity (i.e., small $n(T_B)$) at T_B, and hence, there are little differences between the cooperative α-relaxation time, the primitive α-relaxation time, and the noncooperative β-relaxation time all at T_B (see Figures 1c and 2). In other words, at $T = T_B$, $[\log[\tau_\alpha(T_B)] - \log[\tau_\beta(T_B)] \approx [\log[\tau_\alpha(T_B)] - \log[\tau_o(T_B)] \approx 0$, and thus the interpretation readily explains also why the $\alpha-\beta$ bifurcation temperature, T_β, coincides with T_B, as found experimentally.[5−9]

4. Possible Origin of the Dixon−Nagel Scaling

Dielectric loss data of glass-forming liquids, $\epsilon''(f)$, when plotted as a function of frequency, f, are characterized by the peak frequency, f_p, the normalized width w, and the relaxation strength, $\Delta\epsilon = \epsilon_0 - \epsilon_\infty$. Dixon et al.[12,13] showed that a plot of $w^{-1}\log(\epsilon'' f_p/\Delta\epsilon f)$ vs $w^{-1}(1 + w^{-1})\log(f/f_p)$ collapses dielectric relaxation data from six different glass-formers including glycerol and PG onto a single scaling plot valid over 13 decades of frequency. The same scaling form has since been shown to hold for cyclooctanol[30] and the electric loss modulus of ionic conductors.[38] Up to now the success of the Dixon−Nagel scaling has not been explained although it has been subjected to several interpretations and criticisms.[39−41] In view of our current proposed interpretation of the structure of the dielectric relaxation spectrum and the relations between the α-relaxation, the primitive α-relaxation, and the β-relaxation in glass-formers, it is natural to test whether this picture can explain the Dixon−Nagel scaling or not.

The test is carried out by approximating $\tau_\beta(T)$ by $\tau_0(T)$, which we have shown above to be valid, and simulating dielectric spectra using different values of n and τ_α over a broad frequency range. τ_0 can be calculated from τ_α by eq 8 because n has been specified. Later we shall investigate how sensitive the Dixon−Nagel scaling is to different choices of the ratio $\tau_\beta(T)/\tau_0(T)$. As we have already mentioned in the above, the dielectric relaxation spectrum of some of these glass formers can be fitted by using two superimposed relaxation functions. A KWW function or a Cole−Davidson function is used to describe the α-relaxation, and an additional Cole−Cole function to account for the β-relaxation, which is assumed to be always present although its peak cannot be resolved and only gives rise to the observed high-frequency wing. Therefore, the dielectric relaxation data can be described by

$$\epsilon^*(\omega) - \epsilon_\infty = \frac{\Delta\epsilon_\alpha}{(1 + j\omega\tau_\alpha)^\nu} + \frac{\Delta\epsilon_\beta}{(1 + j\omega\tau_\beta)^\sigma} \qquad (9)$$

and this is the expression we have used to simulate different dielectric relaxation spectra. Equation 9 excludes the possible presence of a constant loss contribution to the dielectric response.[42] If this additional term is considered in the fits to experimental data, the parameters obtained for the Cole−Cole function may vary, making the β-relaxation contribution narrower. We shall not consider this term here because its presence does not modify the conclusions of this work, and it will be subject of a future publication. It has been also shown in some glass-formers that, instead of a Cole−Davidson function, a Havriliak−Negami function[43] is needed to describe the α-relaxation of some glass-forming liquids and polymers. In these cases, ϵ'' does not increase linearly with frequency at the low-frequency side of the α-relaxation peak and therefore the Dixon−Nagel scaling fails.[44,45] It has been proposed that the existence of a dc conductivity or other relaxation processes can be responsible of this apparent sublinear dependence of ϵ'' at the lower frequencies, and the Dixon−Nagel scaling of the α-relaxation is obeyed when these additional processes are subtracted.[46,47] We do not consider this possible aberration of the α-relaxation spectrum in this work.

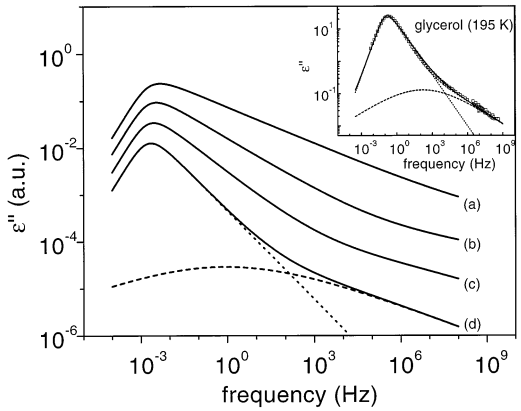

Figure 3. Solid curves representing simulations of dielectric relaxation loss spectra obtained according to eq 9 by a superposition of a Cole−Davidson function and a Cole−Cole function to account for the α- and the β-relaxations, respectively. In all cases $\tau_\alpha = 10^2$s, $\tau_\beta = \tau_0$, and $\Delta\epsilon_\alpha/\Delta\epsilon_\beta = 100$. The exponent ν is different for each curve to simulate different widths w of the α-relaxation: (a) $w^{-1} = 0.5$; (b) $w^{-1} = 0.6$; (c) $w^{-1} = 0.7$; (d) $w^{-1} = 0.8$. The exponent σ has been chosen to satisfy the relation $(1 + \sigma) \approx 0.7(1 + w^{-1})$. The dotted and dashed lines represent the Cole−Davidson and Cole−Cole functions, respectively, for case d, $w^{-1} = 0.8$. Square symbols in the inset are experimental ϵ'' data for glycerol at 195 K, after Lunkenheimer et al. The solid line through the data points is a fit according to eq 9 with $w^{-1} = 0.73$, $\tau_\alpha = 1.55$ s, and $\tau_\beta = \tau_0 = 9.56 \times 10^{-4}$ s, and the dotted and dashed lines are the corresponding Cole−Davidson and Cole−Cole functions obtained in the fit.

Four different simulated curves using $\tau_\alpha = 10^2$ s and four different values of w^{-1} equal to 0.5, 0.6, 0.7, and 0.8 are presented in Figure 3. In the following, we explain the criteria used in the simulations to choose the parameters in eq 9 in order to account for the spectral dispersions experimentally observed in different glass-formers. In the inset of Figure 3 experimental dielectric relaxation data of glycerol near the glass transition measured by Lunkenheimer et al.[32] are reproduced. In the inset, we have also included the fit according to eq 9 and the constraint $\tau_\beta = \tau_0$. The dotted and dashed lines are the corresponding Cole−Davidson and Cole−Cole functions used in the fit. The exponent ν of the Cole−Davidson function defines the normalized width w of the α-relaxation, which is the parameter used in the Dixon−Nagel scaling to characterize the non-Debye relaxation behavior, and it is related to the coupling parameter n (see eq 3). The exponent σ of the Cole−Cole function accounts for the slope of $\epsilon''(\omega)$ in a log−log plot at the higher frequencies. The different glass-forming liquids that have been proved to scale in this way show different widths between 1.17 and 2.2, and in all cases the exponent σ has been shown[33] to be empirically related to w by the relation $(1 + \sigma) \approx 0.7(1 + w)$. Therefore, we have simulated dielectric spectra by choosing different values of the exponents ν and σ covering the different values of w experimentally obtained and satisfying the relation above. We can see also from the inset of Figure 3 that the amplitude of the α-relaxation loss peak is about a factor of 100 larger than that of the β-relaxation peak. Although τ_β is not exactly the same as τ_0, they are not far apart at the glass

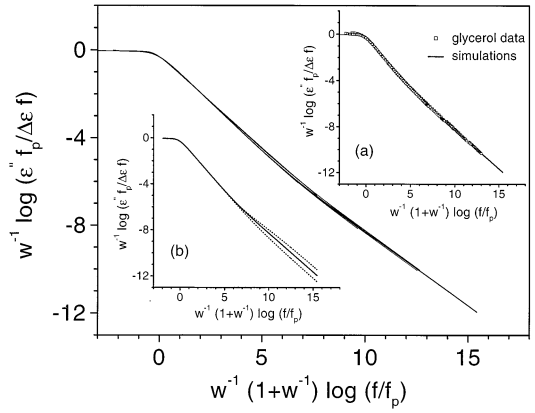

Figure 4. Main figure: Dixon−Nagel scaling plot for several dielectric spectra simulated by using eq 9 with $\tau_\beta = \tau_0$ as explained in the text. The curves in the main figure are obtained from 10 simulations using different values for τ_α and w as follows: $\tau_\alpha = 10^4$ s and $w^{-1} = 0.5$, $w^{-1} = 0.6$, $w^{-1} = 0.7$, $w^{-1} = 0.8$; $w^{-1} = 0.5$ and $\tau_\alpha = 10^2$ s, $\tau_\alpha = 1$ s, $\tau_\alpha = 10^{-2}$ s; $w^{-1} = 0.8$ and $\tau_\alpha = 10^2$ s, $\tau_\alpha = 1$ s, $\tau_\alpha = 10^{-2}$ s. The inset a is a Dixon−Nagel plot for the same simulations of the main figure and for glycerol data at 184, 195, 213, and 223 K (all represented by open squares), after Lunkenheimer et al. Inset a shows that in the scaling plot the simulated curves and experimental data are indistinguishable from each other. Inset b is a Dixon−Nagel plot for three simulations using $w^{-1} = 0.8$ and $\tau_\alpha = 10^4$ s but with different τ_β/τ_0 ratios. The solid line, which is also included in the main figure, is obtained for $\tau_\beta = \tau_0$. The two dotted lines, which violate the Dixon−Nagel scaling, are obtained for τ_β a factor 10^3 times larger and smaller than τ_0.

transition temperature as it has been shown in all cases where the β-relaxation has been resolved. As we have seen from the example of OTP in Figure 1c and cyclooctanol in Figure 3a, $\tau_\beta(T) \approx \tau_0(T)$ at temperatures higher than T_g, particularly in the vicinity of T_B. Therefore the constraint $[\tau_\beta(T)/\tau_0(T)] = 1$ together with the choice $\Delta\epsilon_\alpha/\Delta\epsilon_\beta = 100$ seems to be a reasonable in simulating the dielectric relaxation spectra of glass-forming liquids by using eq 9. Other choices of the two ratios have been examined and similar results have been obtained.

We have performed the Dixon−Nagel scaling on several simulated dielectric spectra using different values of w^{-1} from 0.5 to 0.8 and different values of the α-relaxation time, τ_α, in the range 10^{-4}−10^4 s, and the scaled curves are presented in Figure 4. All the simulations have been made with the constraint that $\tau_\beta = \tau_0$. It can be observed that all the curves are very close to and indistinguishable from each other, although they do not exactly collapse onto a single master curve. We have superimposed these scaled simulated curves onto the scaled experimental dielectric data of glycerol at different temperatures.[32] The result shown in inset (a) in Figure 4 indicates that all the scaled simulated curves are indistinguishable from the Dixon−Nagel scaled data of glycerol and other glass-formers. However, if τ_β is chosen to be very different from τ_0 to obtain the simulated curves, the Dixon−Nagel scaling is not obeyed. The solid curve in inset b in Figure 4 corresponds to simulations for $(1 - n) \approx w^{-1} = 0.8$, $\tau_\alpha = 10^4$ s, and $\tau_\beta = \tau_0$. The two dotted are scaled simulated data with the same choice of $(1 - n) \approx w^{-1} = 0.8$ and $\tau_\alpha = 10^4$ s, but now τ_β is a factor 1000 larger and smaller than τ_0. These results indicate that the success of the Dixon−Nagel scaling can be rationalized by the proposed relation between the α- relaxation, the primitive α-relaxation, and the β-relaxation shown in previous sections of this work.

5. Conclusion

The temperature dependence of the α-relaxation time from either dielectric and viscosity measurements over an extended range is quite complicated. In some glass-formers[5−8] there are three distinguishable temperature dependencies, the high-temperature truly Arrhenius dependence and the two VFT dependencies at lower temperatures discussed in this work. While it would be extremely difficult to come up with a quantitative explanation of the complicated temperature dependence, the changes of various quantities across T_B, the correlation between them, and the coincidence of T_B and T_β offer sufficiently a challenge to be explained. Each of these properties is interesting, but appearing all at one time, they pose a problem of identifying which one is more fundamental and the cause of the others as effects. From the results of our analysis of the experimental data and comparison with the predictions of the coupling model, we make the conclusion that the rapidity of the change of the coupling parameter, n, or the Kohlrausch exponent, $(1 - n)$, is the origin of all other observed properties. From the rapidity of the change of n across T_B and the size of its maximum value attained at T_g, the coupling model can explain the trends found in the other properties of the α- and β-relaxations. In this manner, the near coincidence of T_B and T_β, the shape of the dielectric spectra of small-molecule glass-formers at temperatures above T_g, and the origin of their Dixon−Nagel scaling property can be explained.

Acknowledgment. The work is supported by the Office of Naval Research. The stay of C.L. at The Naval Research Laboratory is made possible by a NATO Fellowship. We thank R. Brand, P. Lunkenheimer, and R. Richert for making their original data available to us. Special thanks to P. Lunkenheimer for stimulating discussions.

References and Notes

(1) See collection of papers in: *J. Non-Cryst. Solids* **1991**, *131−133* (Ngai, K. L., Wright, G. B., Eds.). *J. Non-Cryst. Solids* **1994**, *172−174* (Ngai, K. L., Riande, E., Wright, G. B., Eds.). *J. Non-Cryst. Solids* **1998**, *235−238* (Ngai, K. L., Riande, E., Ingram, M., Eds.).

(2) See collection of papers in: *Supercooled Liquids, Advances and Novel Applications*; Fourkas, J. T., et al., Eds.; ACS Symposium Series 676; American Chemical Society: Washington, DC, 1997.

(3) Ngai, K. L. *Comments Solid State Phys.* **1979**, *9*, 121. Ngai K. L.; Rendell, R. W. In *Supercooled Liquids, Advances and Novel Applications*; Fourkas, J. T., et al., Eds.; ACS Symposium Series 676; American Chemical Society: Washington, DC, 1997; p 45.

(4) Tsang, K. Y.; Ngai, K. L. *Phys. Rev. E* **1996**, *54*, R3067. Tsang, K. Y.; Ngai, K. L. *Phys. Rev. E* **1997**, *56*, R17.

(5) Stickel, F.; Fischer, E. W.; Richert, R. *J. Chem. Phys.* **1996**, *104*, 2043.

(6) Stickel, F. Ph.D. Thesis, Mainz University, Shaker, Aachen, Germany**,** 1995.

(7) Hansen, C.; Stickel, F.; Berger, T.; Richert, R.; Fischer, E. W. *J. Chem. Phys.* **1997**, *107*, 1086.

(8) Hansen, C.; Stickel, F.; Richert, R.; Fischer, E. W. *J. Chem. Phys.* **1998**, *108*, 6408.

(9) Richert, R.; Angell, C. A. *J. Chem. Phys.* **1998**, *108*, 9016.

(10) Kohlrausch, R. *Pogg. Ann. Phys.* **1847**, *12* (3), 393.

(11) Williams, G.; Watts, D. C. *Trans. Faraday Soc.* **1970**, *66*, 80.

(12) Dixon, P. K.; Wu, L.; Nagel, S.; Williams, B. D.; Carini, J. P. *Phys. Rev. Lett.* **1990**, *65*, 1108.

(13) Dixon, P. K. *Phys. Rev. B* **1990**, *42*, 8179.

(14) Böhmer, R.; Ngai, K. L.; Angell, C. A.; Plazek, D. J. *J. Chem. Phys.* **1993**, *99*, 4201.

(15) (a) Wagner, H.; Richert, R. *J. Phys. Chem. B* **1999**, *103*, xxxx. (b) Steffen, W.; Patkowski, A.; Glaesser, H.; Meier, G.; Fischer, E. W. *Phys. Rev. E* **1994**, *49*, 2992. Steffen, W. Ph.D. Thesis, Mainz University, Shaker, Aachen, Germany, 1993.

(16) Ngai, K. L. *Phys. Rev. E* **1998**, *57*, 7346.

(17) Johari, G. P.; Goldstein, M. *J. Chem. Phys.* **1970**, *53*, 2372.

(18) Colmenero, J.; Arbe, A.; Alegria, A. *Phys. Rev. Lett.* **1993**, *71*, 2603. Ngai, K. L.; Colmenero, J.; Arbe, A.; Alegria, A. *Macromolecules* **1992**, *25*, 6727.

(19) Zorn, R.; Arbe, A.; Colmenero, J.; Frick, B.; Richter, D.; Buchenau, U. *Phys. Rev. E* **1995**, *52*, 781.

(20) Roland, C. M.; Ngai, K. L.; Lewis, L. *J. Chem. Phys.* **1995**, *103*, 4632.

(21) Roe, R.-J. *J. Chem. Phys*. **1994**, *100*, 1610. Ngai, K. L. *J. Chem. Phys*. **1993**, *98*, 7588.
(22) Smith, G. D.; Paul, W.; Yoon, D. Y.; Zirkel, A.; Hendricks, J.; Richter, D. *J. Chem. Phys*., in press.
(23) Roe, R.-J. *J. Non-Cryst. Solids* **1998**, *235*−*238*, in press.
(24) Ngai, K. L.; Cramer, C.; Saatkamp, T.; Funke, K. In *Non-Equilibrium Phenomena in Supercooled Fluids, Glasses and Amorphous Materials*; Giordano, M., Leporini, D., Tosi, M. P., Eds.; World Scientific: Singapore, 1996; p 3.
(25) Garwe, F.; Beiner, M.; Hempel, E.; Schawe, J.; Schröter, K.; Schönhals, A.; Donth, E. *J. Non-Cryst. Solids* **1994**, *172*−*174*, 191.
(26) Perez, J.; Cavaille, J. Y.; Etienne, S.; Fouquet, F.; Guyot, F. *Ann. Phys., Fr*. **1983,** *8*, 417.
(27) Fujimori, H.; Oguni, M. *Solid State Commun*. **1995**, *94*, 157.
(28) Kudlik, A.; Tschirwitz, S.; Benkhof, S.; Blochhowicz, T.; Roessler, E. *Europhys. Lett*. **1997**, *40*, 649.
(29) Angell, C. A. In ref 2, p 14.
(30) Leslie-Pelecky, D. L.; Birge, N. O. *Phys. Rev. Lett*. **1994**, *72*, 1232.
(31) Brand, R.; Lunkenheimer, P.; Loidl, A. *Phys. Rev. B* **1997**, *56*, R5713.
(32) Lunkenheimer, P.; Pimenov, A.; Dressel, M.; Goncharov, Yu G.; Böhmer, R.; Loidl, A. *Phys. Rev. Lett*. **1996**, *77*, 318.
(33) Leheny, R. L.; Nagel, S. R. *Europhys. Lett.* **1997**, *39*, 447.
(34) Leheny, R. L.; Nagel, S. R. *J. Non-Cryst. Solids* **1998**, *235*−*238*, in press.
(35) Cole, K. S.; Cole, R. H. *J. Chem. Phys*. **1941**, *9*, 341.
(36) Davidson, D. W.; Cole, R. H. *J. Chem. Phys*. **1951**, *19*, 1485.
(37) Lunkenheimer, P.; Ngai, K. L., Unpublished data.
(38) Leon, C.; Lucia, M. L.; Santamaria, J.; Sanchez-Quesada, F. *Phys. Rev. B* **1998**, *57*, 41.
(39) Kudlik, A.; Benkhof, S.; Lenk, R.; Rossler, E. *Europhys. Lett.* **1995**, *32*, 511.
(40) Dendzik, Z.; Paluch, M.; Gburski, Z.; Ziolo, J. *J. Phys. Condens. Mater*. **1997**, *9*, L339.
(41) Chamberlin, R. V. *J. Non-Cryst. Solids* **1997**, *215*, 293.
(42) Ngai, K. L.; Moynihan, C. T. *Bull. Mater. Res. Soc*. **1998**, 23, No. 11, 51.
(43) Havriliak, S.; Negami, S. *Polymer* **1967**, *8*, 161.
(44) Schönhals, A.; Kremer, F.; Schlosser, E. *Phys. Rev. Lett*. **1991**, *61* (8), 999.
(45) Kudlik, A.; Benkhof, S.; Lenk, R.; Rossler, E. *Europhys. Lett*. **1995**, *32*, 511.
(46) Menon, N.; Nagel, S. R. *Phys. Rev. Lett*. **1993**, *71* (24), 4095.
(47) Schönhals, A.; Kremer, F.; Stickel, F. *Phys. Rev. Lett.* **1993**, *71*, 4096.